Comparing Convective Weather Impacts on Air Traffic Management Operations in United States, Canada & Europe

Gabriele Enea[1], Tom Reynolds[1], Joseph Venuti[1], Tatiana Polishchuk[2], Valentin Polishchuk[2], Anastasia Lemetti[2], Alexander Lau[3], Julian Solzer[3] and Tobias Bölle[3]

[1]MIT Lincoln Laboratory
[2]Linkoping University
[3]DLR German Aerospace Center

Abstract

Adverse weather is the primary cause of delays to air traffic. In this paper models of different maturity level from the United States, Canada and Europe are compared to derive best practices in how to mitigate these impacts. The models are illustrated through case studies in each one of these airspaces. An example in Jacksonville Center in Florida, one for Toronto Airport and one for the Rhein Airspace adjacent to Munich Airport are presented here. Lastly, some of the modeling characteristics are compared to derive best practices and lesson learned that can be leveraged from each other.

Keywords: weather impacts; decision-support tools; convective weather.

1. Introduction

Challenging weather such as thunderstorms, winds and turbulence is the major source of air transportation delays [1]. This is especially impactful in the United States, Canada and Europe due to challenging weather types [2] and high traffic levels. If not effectively forecasted, weather impacts translate into inefficiencies in the system. For example, according to a Eurocontrol 2021 study, bad weather forced airlines to fly one million extra kilometers, burning more than 6,000 tons of extra fuel and producing more than 19,000 tons of CO_2 [3].

Further understanding weather challenges and effective mitigations to them in the United States, Canada and Europe will be especially important as air traffic continues to grow and weather challenges evolve. A recent report from the European Aeronautical Safety Agency (EASA) [4] makes initial projections of potential weather changes in the future. For example, in Figure 1 the report shows that severe thunderstorms are projected to increase in the United States mostly along the East Coast and Gulf of Mexico (darker red), while estimates for the European continent show a more mixed picture, with some increases in the Mediterranean (dark red) and reductions in parts of Northern Europe (blue). Regardless of future projections, given that the air traffic management system is increasingly global, there is a need to compare and contrast how weather impacts are mitigated now and leverage best practices and models developed in different parts of the world.

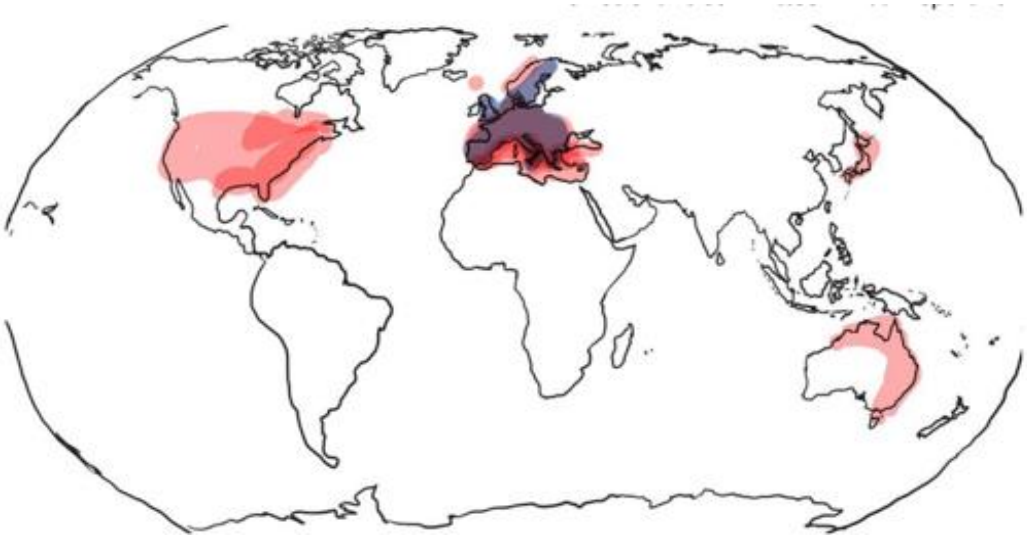

Figure 1 - Severe thunderstorm future projections [4]. Blue and red represent a negative and a positive trend, respectively.

This paper compares weather models that can be used in Decision-Support Tools (DSTs) to help controllers and traffic managers in mitigating the impacts of convective weather. First a high-level methodology is described in Section 2. To illustrate the methodology, case studies are presented in Section 3 for weather impact examples from the United States, Canada and Europe. The paper is concluded by a comparison of the different approaches, summary and conclusions in Section 4.

2. Methodology

Given the current and future weather-related challenges that the air transportation system will be facing, this paper presents an initial study to compare and contrast major weather challenges in the United States, Canada and Europe, identifying best practices, gaps in aviation weather technology and lessons learned that can be leveraged from each other's experience. This will be done by focusing on approaches to identify weather impacts on airspace capacity, which is a major factor affecting smooth operations in all these airspaces.

The study started with identifying the major impacts of weather at key airports in the United States, Canada and Europe, some of these impacts are projected to grow. Case studies of busy airports/airspace with weather challenges were identified first. The airspace in Jacksonville control center in the US, Toronto Pearson airport and airspace in Canada, and Rhein upper airspace (UIR) as an airspace on top of the arrival and departure airspaces of Munich International airport in Germany were selected because of the specific local weather impacts that affect these busy airspaces.

Best practices to mitigate the impact of weather events on air traffic in the study regions will be discussed and lessons learned in terms of technology, weather models, and operational procedures will be compared and contrasted. Examples of best practices include what weather forecast models, decision support tools and operational techniques are being used, which are most effective and how they might apply or be adapted for use in wider ATC operations. Furthermore, three convective weather models and relevant weather decision-support tool, one for each airspace, will be described.

Lastly, lessons learned will be summarized to benefit the entire ATM community, by identifying gaps which could be addressed by new technologies and/or procedures.

3. Case Studies

In this section, three case studies from different airspaces around busy airports in the study regions are presented. These were selected for different reasons that will be described in each sub-section.

3.1 Florida Airspace and Airports

In the United States, the airspace of Jacksonville Center (ZJX) has seen an increase in flight demand after the COVID pandemic and is often subject to severe convective storms, especially in the summer

years [5]. These two factors combined have caused significant additional delays in recent years. When convective weather impacts the airspace capacity in ZJX, the FAA applies restrictions called Airspace Flow Programs (AFPs) which are similar to Ground Delay Programs (GDPs) but applied to the airspace. These are denominated. Before the COVID pandemic, these programs were used only during 10 days in the convective season of 2019, while in the convective season of 2023 these programs were implemented on 46 days. This increase was driven by multiple factors but mostly by the increase in demand that ZJX airspace has experienced. After a spike in number of days with AFPs in 2022, the number went down in 2023, showing also an improvement in the total number of delay minutes that was introduced into the system to mitigate the impacts of weather. The total minutes of delays imposed by AFPs and GDPs in ZJX are presented in

Table *1*. These delays are not all to flights traversing ZJX airspace, but they could be applied to flights going from the north-east to Florida that were held at the departing airport due to an AFP in ZJX.

Table 1 - Weather impacted days in ZJX when AFPs were implemented and total delays [5].

AFP Usage	**2019 [Days]**	**2021 [Days]**	**2022 [Days]**	**2023 [Days]**
Total	10	17	55	46
Tot ZJX Ground Delays (GDPs + AFPs) [mins]	440,417	968,816	2,852,051	2,418,787

To illustrate the weather impacts and mitigations, a representative day impacted by the typical weather in ZJX was selected from June 15, 2023. A major convective system with large convective weather cells impacted the northern ZJX airspace, which is key for traffic to reach busy airports in Florida. Two such airports are Miami International (MIA) and Tampa Airport (TPA) shown in Figure *2*. Pilots need to avoid these storm areas to maintain safety and therefore the capacity of the impacted airspace is reduced. To mitigate these impacts, the FAA implemented multiple AFPs. On June 15, three AFPs were implemented: ZJX1, JY3 and JG5, which are represented by the white lines in Figure *2*. MIT Lincoln Laboratory has created airspace evaluation areas that roughly align with AFPs that can be used by air traffic managers to evaluate the current and future weather impacts with a stop light chart approach in 60 minute intervals. These impacts, red (high), yellow (medium) and green (low/none) are provided by the Traffic Flow Impact (TFI) model [6] and are visible in the bottom of Figure *2*. The evaluation boxes which are closest to the ZJX1, JY3 and JG5 flow constrained areas used in the AFPs are represented by the dotted cyan boxes in Figure *2*. MIT LL maintains historical data of TFI-predicted impact data that were used for this analysis.

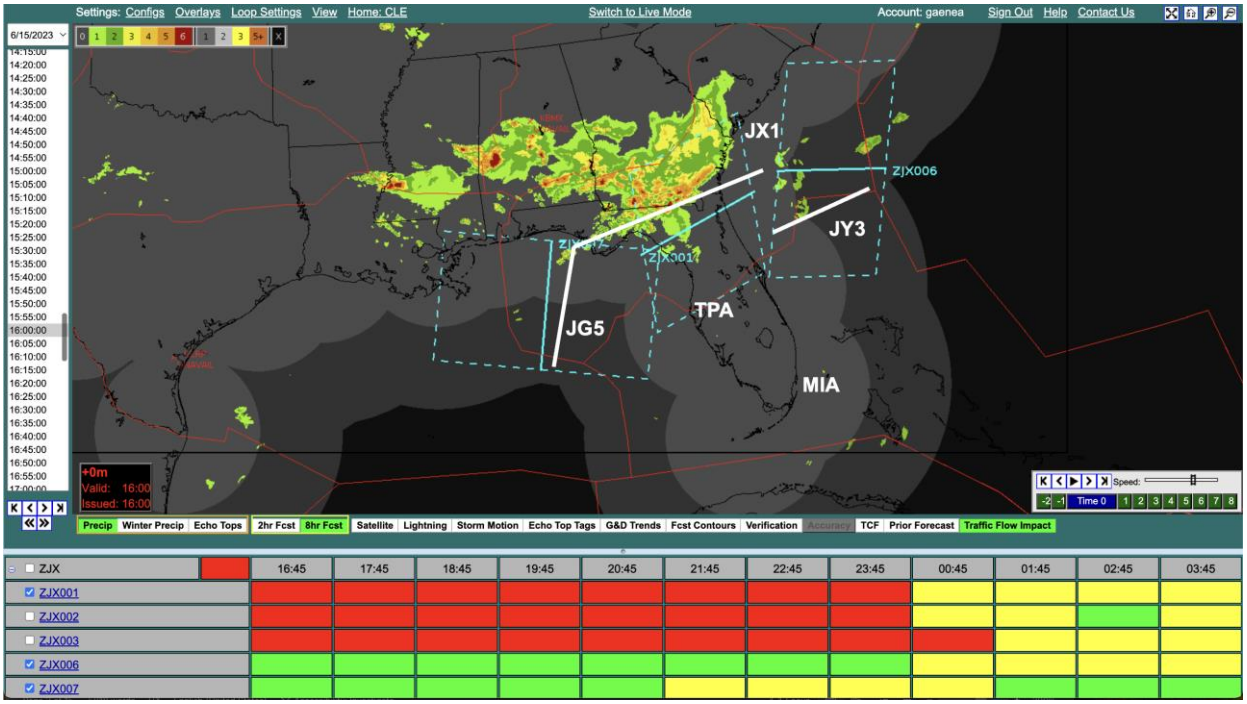

Figure 2 - June 15, 2023 TFI interface at 1600Z with overlayed implemented AFPs.

The main impact metric produced by TFI is the airspace permeability, with 100% corresponding to airspace free of weather impacts, 0% is an airspace completely blocked by weather. Figure *3* shows the permeability predicted on June 15 at 1600Z for the ZJX001 box; this box roughly corresponds to the ZJX1 AFP control area. TFI was predicting very high impacts lasting until 0000Z, with the 20th-80th percentile uncertainty represented by the shaded blue area around the blue dotted line in Figure *3*. More information about the permeability metric and the uncertainty can be found in [6].

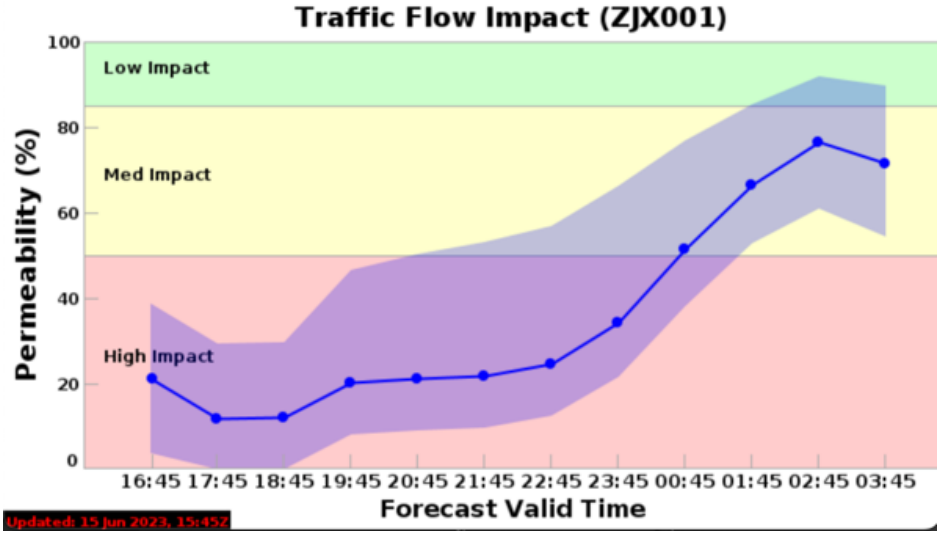

Figure 3 – Permeability vs Forecast time predicted by TFI (blue line) and uncertainty bound (shaded blue).

TFI is a prototype system that is available to many Traffic Managers in the United States through the Consolidated Storm Prediction for Aviation (CoSPA) website to help plan for weather impact mitigation strategies, especially to plan AFPs. When these programs are necessary in ZJX, the capacity of the airspace is highly reduced by weather. Key decisions are on the amount of reduced capacity, and therefore on the program hourly rate and duration. According to the TFI permeability predictions, on June 15 the ZJX1 program should have started with low hourly rates and then progressively increased them around 2300Z. This is what the FAA Traffic Mangers planned for by starting with a 50 aircraft per hour rate, and increasing it progressively to 90 for the last hour of the program (0100Z June 16 in Table *2*).

Table 2 - June 15, 2023 AFP hourly rates.

	FCAJX1	FCAJY3	FCAJG5
18Z	50		30
19Z	50	33	26
20Z	50	26	26
21Z	50	33	26
22Z	70	33	26
23Z	80	22	26
00Z	80	14	19
01Z	90	20	35
02Z		20	9
03Z			10
04Z			20

The other two programs, JY3 and JG5, needed to be revised because the rates initially planned were not achievable given how the weather evolved over the Gulf of Mexico and the Atlantic Routes. It should be noted that the JG5 and JY3 regions cover a smaller piece of airspace and therefore they can process lower hourly rates of flights compared to JX1.

Historical data from FAA records in the Aviation System Performance Metrics (ASPM) database [7] shows that, during these programs, Tampa (TPA) and Miami (MIA) airports were severely impacted and could not process their arrival and departure demand even if the weather never reached the two airports directly. This shows how important ZJX airspace is for effective operations in busy airports in the south of Florida and therefore how mitigations applied by the FAA to reduce the airspace demand directly affect the airports' ability to process their arrival and departure demand.

3.2 Toronto Airport

Toronto Pearson (YYZ) is the busiest airport in Canada and is subject to convective weather in the summer and challenging winds and snowstorms in the winter. A variety of airport and terminal/enroute airspace capacity prediction tools are being prototyped at the airport as summarized in [8]. This paper focuses on the terminal technology, called the Terminal Capacity Evaluation and Prediction Tool (TCEPT). TCEPT predicts terminal airspace and fix (also known as "bedpost") availability and capacity to guide strategic and tactical planning in convective weather. This will allow proactive re-routing of arrivals and departures to available fixes and more effective conditioning of arrival demand for transitioning to time-based arrival management during convective weather. The TCEPT prototype is being developed initially for Toronto Pearson airport and the display currently available to users is shown in Figure *4*. TCEPT is based on similar underlaying algorithm as TFI and the similarity can be seen with the impact plots shown in Figure *3* and Figure *4*.

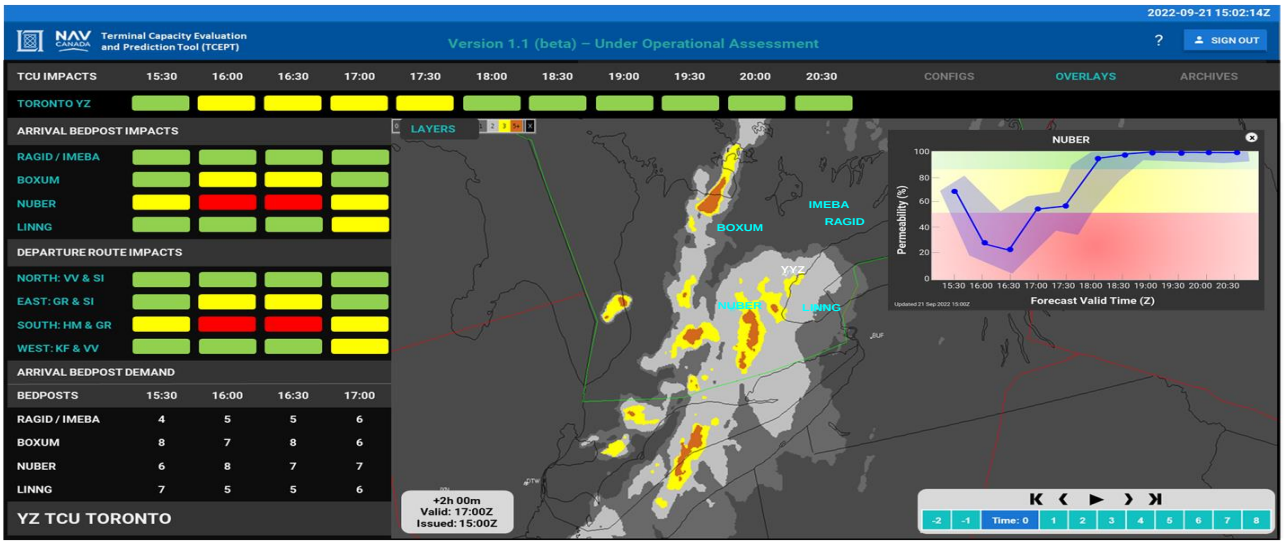

Figure 4 – TCEPT prototype display.

It currently comprises a 0-8 hour weather forecast situational awareness display based on CoSPA zoomed into the YYZ terminal area. The arrival bedposts (named IMEBA, RAGID, LINNG, NUBER and BOXUM) are visible in cyan text within the weather display. The left side of the TCEPT display provides a tabular representation of the weather impacts on the terminal region, where the rows of the table are each bedpost (as well as a row for the overall Terminal Control Unit (TCU)), and the columns are times into the future in 30 minute time bins. Additionally, TCEPT provides estimated bedpost arrival demand over the next 2 hours (see panel at the bottom left of Figure *4*) utilizing a combination of radar-derived aircraft data and flight plan message data. This combination of predicted convective weather impact and arrival demand allows users to thoroughly evaluate potential flight over-delivery situations and plan mitigations accordingly. For the day shown, convective weather is moving into the terminal area from the west to east and the south-west bedpost (NUBER) is being impacted over the next few hours as shown by the yellow and red impact colors in the cells of the display. By clicking on a bedpost, TCEPT also provides a graphical representation of the estimated permeability of the terminal airspace around it over the available forecast horizon. Permeability, as discussed in Section 3.1, represents the degree to which traffic flows are constrained by convective weather in a given airspace region. Permeability is translated into a categorical impact metric (e.g., low/green, moderate/yellow, severe/red) or a quantitative measure of the achievable or sustainable traffic flow rates. These can be generated through a large statistical analysis of historical traffic flow rates, which can then be used to estimate capacity. This uses the same general methodology as the TFI technology described in the previous section, but adapted for the descending flight tracks through wedge-shaped airspace regions feeding each terminal bedpost. In the sample profile in the figure, the weather impacts to NUBER over the next several hours are clearly visible, followed by recovery in the permeability as the weather moves away. This graph also displays 20th-80th percentile uncertainty bounds around the estimates so users can factor the confidence levels of the estimates into their decision-making. In order to illustrate how this technology can be used to manage operations in the terminal area during a convective weather event, Figure *5* illustrates four time snapshots of a case day from August 2023 when convective weather moved through the Toronto area. The left panel for each time shows a snapshot of the arrival and departure flight paths, while the right panels show the corresponding TCEPT display.

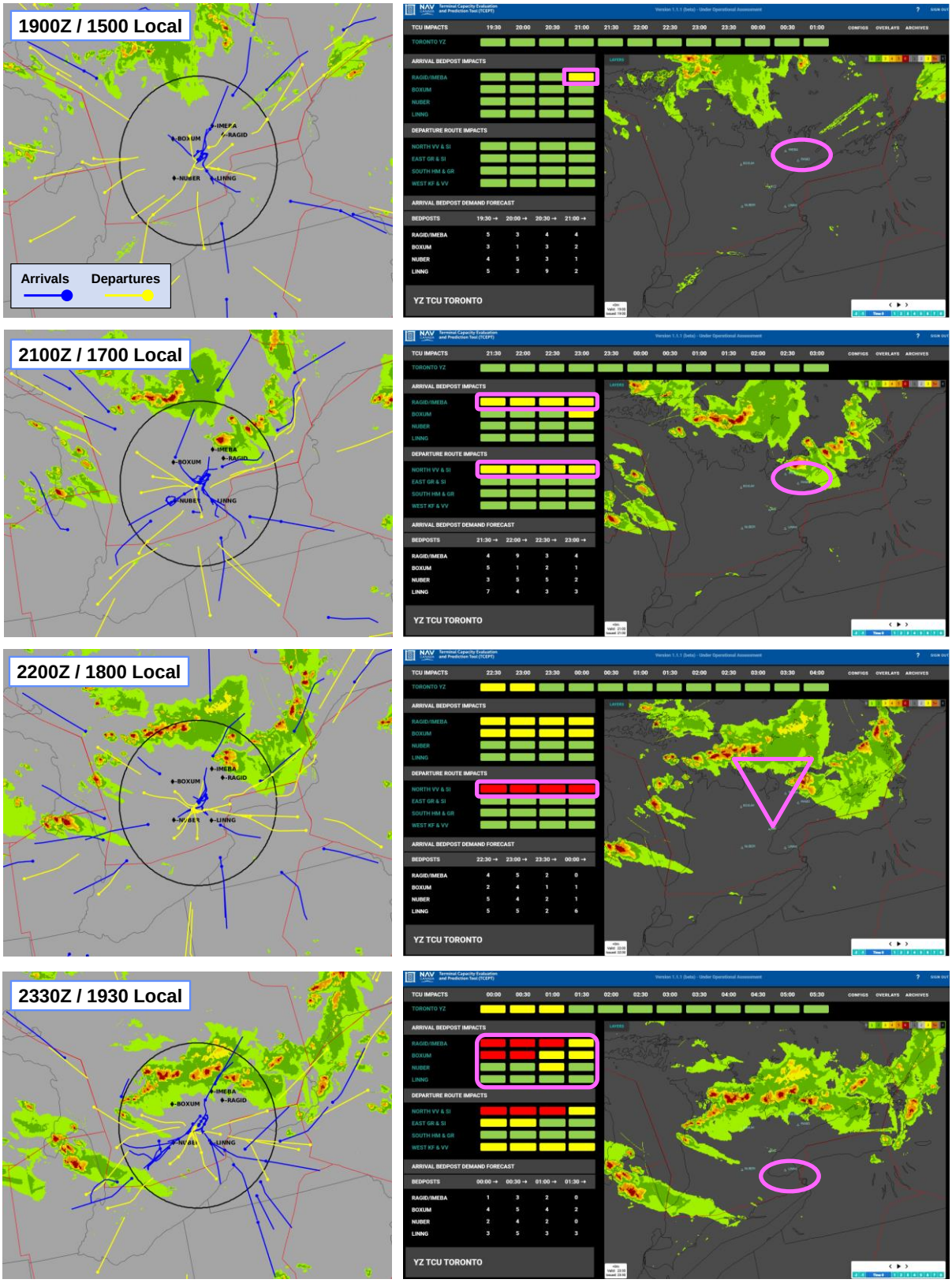

Figure 5 – Case study of TCEPT usage during convective weather event.

At 1900Z, weather activity can be seen moving in from the north-west of the airport. TCEPT is predicting a yellow weather impact over the RAGID/IMEBA bedposts (those north-east of the airport) in two hours' time (i.e., at 2100Z). Traffic flow in and out of the airport bedposts is normal at this time, but this is the first indication to terminal controllers of potential impacts in the future. Two hours later at 2100Z, the RAGID/IMEBA bedposts are now showing yellow impacts extending at least the next two hours, while the northern departure routes are now showing impact as well as the weather moves further east and intensifies. The traffic flows are showing evidence of controllers having to tactically deviate flight tracks in order to avoid the weather, but are still largely able to cross the bedposts just

downstream. At 2200Z, yellow weather impacts are occurring out two hours at the RAGID/IMEBA and BOXUM (north-west) bedposts, while the northern departure routes are now showing red weather impacts over the next two hours. The flight tracks show that departures to the north are now largely blocked and arrivals from the north-east are deviating so much they are no longer crossing the bedposts themselves. TCEPT also shows that at the same time, the other arrival and departure bedposts have much lower weather impacts (green cells), providing alternate routing options for terminal controllers. As the weather gets worse over the northern (RAGID/IMEBA and BOXUM) arrival bedpost, by 2330Z the controller are now utilizing the clearer routes to the south by deviating the arrivals from the north-east over to the south-east bedpost (LINNG).

Because of these weather impacts, the airport eventually had to go into a Ground Stop that lasted between 0015Z and 0130Z (the next day). This was necessary to temporarily pause arriving flights that had not taken off yet, and process those that were already en route to the airport. This case study illustrates how weather forecasts translated into bedpost impacts can be used to more proactively manage traffic and utilize available terminal capacity as efficiently as possible during challenging weather conditions.

3.3 Rhein Upper Information Region (UIR) and Munich Airport

In this section, a case day for Munich International Airport (MUC) and surrounding airspace is presented. Unlike the previous two cases, the weather impact model presented here was developed *ad hoc* for this paper. MUC in 2019 was one of the busiest in Europe with 48 million passenger movements and nearly 20 million air freight tons. The summer months of June and July were particularly affected by thunderstorm-related restrictions, with more than 12,000 minutes of delays per month [9].Thunderstorms very quickly lead to interruptions of flight operations, as ground handling is completely suspended if there is lightning less than three nautical miles from the airport.

The runway system consists of two independent runways 26R/26L, and respectively 08R/08L. The Terminal Maneuvering Area (TMA) is structured according to two main approach directions, north and south, with corresponding runways. Transitions from upper airspace are formed by a path stretching area and take about 12 minutes from the Initial Approach Fix (IAF). If there is no capacity shortfall throughout the day, the runways are usually operated in mixed mode.

Due to two climate zones impacting this region (Atlantic climate and continental climate), there is a special meteorology for the airport and the airspace above it. Particularly in the summer months, when moist air masses from the Atlantic move towards the foothills of the Alps, strong thunderstorm fronts sometimes form in the plains north of the Alps near the airport. These low-pressure areas accumulate in the Alps, resulting in airport impacts caused by heavy rainfall, hurricane force winds and hail. Sometimes, these thunderstorms can reach the upper airspace. Depending on the approach direction and the location, as well as growth and decay of convective cells within the vicinity of the airport, different operational airspace usage is employed. For example, flights are separated vertically to be able to sort arriving aircraft more efficiently before sending them to the final approach path avoiding convective cells. Moreover, operationally within the TMA, when independent arrival flows are used into both runways, it is necessary to activate additional controller positions, and when visibility conditions decrease, the runways are operated individually, one for arrival and one for departure operations.

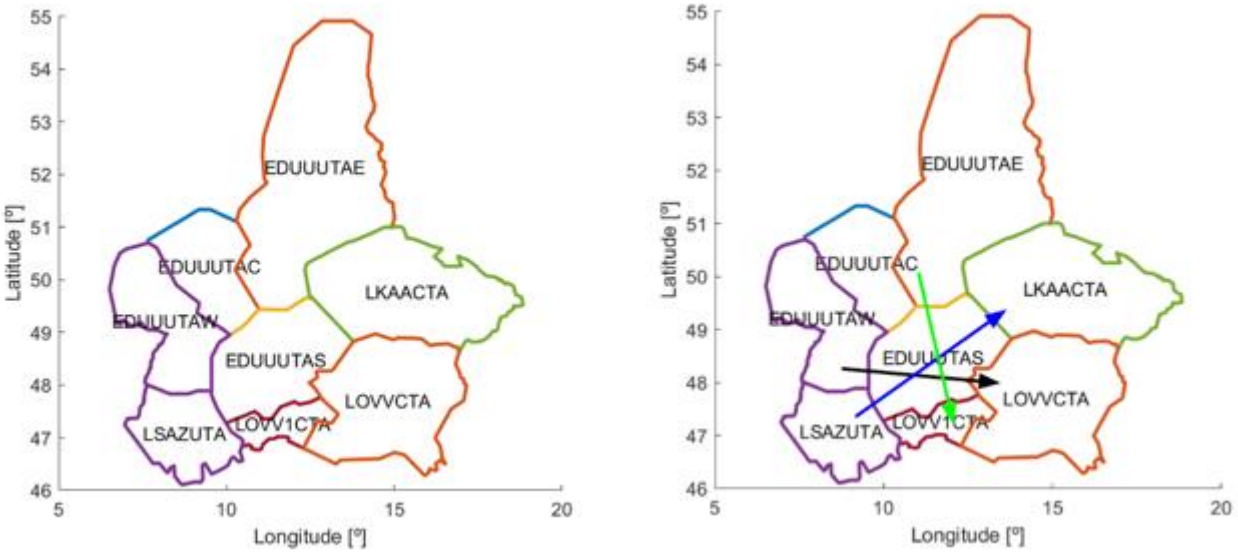

Figure 6 - Left: configuration of the upper airspace of Rhein UIR. Right: Example flows through EDUUUTAS.

Figure 6 shows the sectors configuration of the upper airspace controlled by Rhein UIR. The focus of this case study was the upper-level sector group EDUUUTAS, consisting of sectors EDUUDON, EDUUISA, EDUUALP and EDUUCHI, from FL315 (lower level) to unlimited (UNL). During weather-impacted days, this airspace strongly interacts with arrival and departure procedures in Munich airport, especially when strong convective cells above FL315 impact on sequencing procedures as well as on traffic mix between laterally and vertically moving flights.

A case study focused on Rhein UIR and Munich Airport is described here together with some weather impact models that visualize convective cells together with operational arrival and departure routes. Moreover, the quantification of weather impacts on airspace will be addressed using an approach first presented in [10]. The adaptation of the model for the MUC airspace is specifically developed for this paper, therefore it is explained in greater details in what follows..

3.3.1 Airspace Capacity Model

For the Rhein airspace, we modeled the reduction of the airspace capacity using the mincut/maxflow theory [11][14]. Similar to the TFI model presented above, the reduction of the airspace capacity is not a simple function of the weather coverage: the same percentage of airspace area covered with inclement weather may lead to drastically different possible traffic flows. Airspace capacity depends on the positions of the storm weather cells in relation to these flows. Therefore, in order to forecast the airspace capacity reduction, one should consider the shape of hazardous weather cells, as well as their spatial distribution. Airspace geometry also plays an important role. Capacity depends on the direction of the flow, i.e., the source/sink edges on the boundary of the airspace sector in consideration through which the traffic enters/exits the airspace. The development of this continuous flow theory and algorithms was motivated by ATM needs, and ATM applications of the geometric flow results are presented in [15] and [16].

When applying the geometric maxflow/mincut theory, an airspace sector (on a single flight level) is represented by a 2D polygonal domain, and hazardous weather is modelled as obstacles which should be avoided by the flow Figure *7*. The aircraft enters the airspace through a portion of its boundary, called the source. The aircraft exits through the portion of the boundary called the sink. The source and the sink split the boundary of the sector into two parts called the bottom *B* and the top *T*. The critical graph of the instance has a vertex for every obstacle, for *B* and for *T*. The edges of the graph connect all pairs of the vertices, and the length of every edge is the distance between the vertices. The capacity of the airspace is defined by the mincut (the bottleneck for the flow) which is determined by the shortest *B*-*T* path in the critical graph.

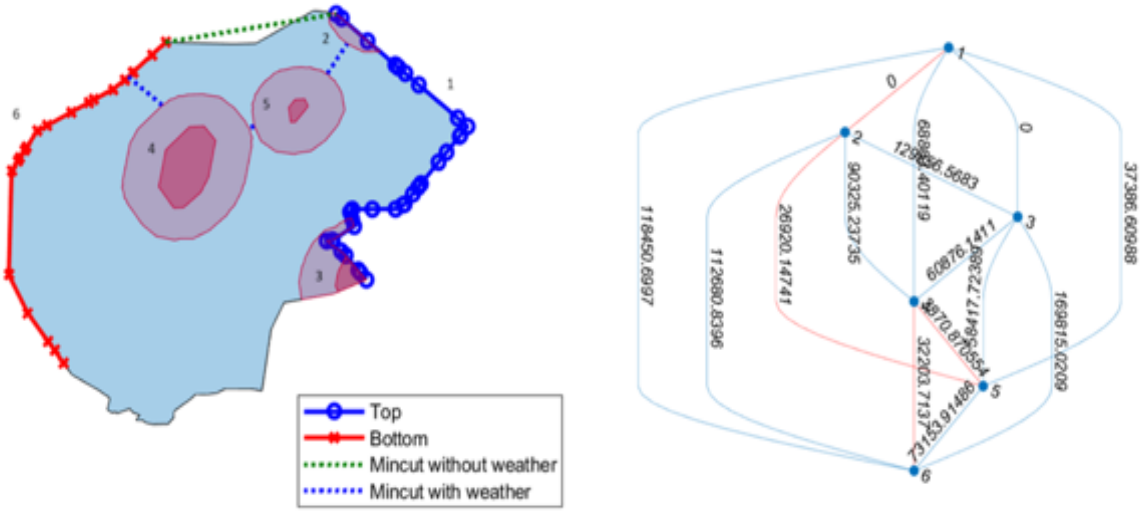

Figure 7 – Left: example of an airspace sector corresponding to EDUUUTAS, with hazardous weather cells (red) at about 1600Z on June 8, 2023; Right: the critical graph; the shortest Bottom-Top path in it (corresponding to the mincut through the sector) is shown in red.

The maxflow/mincut theory assumes that the flow is mostly unidirectional (single source/sink pair) because aircraft with opposing headings are vertically separated. In this paper, we consider the airspace crossed by multiple flows, with different flows entering/exiting through different sources/sinks. This is also similar to the approach used to calculate the permeability metric by TFI, which considers bi-directional flows. The mincuts are therefore computed separately for each source/sink pair. To quantify the capacity reduction, we first calculate the maximum flow capacity of the network assuming no weather constraints. This represents the ideal flow achievable in the absence of weather impacts. Subsequently, the flow capacity is recalculated for the network considering the capacity impacts imposed by convective weather cells. The ratio between the weather-impacted network capacity (W_{mincut}) and the unimpeded network capacity (O_{mincut}) is defined as available flow capacity ratio (*AFCR*) which is utilized as an indicator of the relative degradation in airspace capacity due to convective weather [11].

While in [10] the extended methodology for probabilistic capacity reduction was developed, in this work we use the baseline capacity estimation [[12], [15]] which assumes that the obstacles are deterministic per time stamp, i.e., that their shapes and locations were known exactly for a fixed time period. We take the methodology presented in [12] as a base, but unlike in [12], where the capacity reduction was estimated for the overlayed square grid cells, we forecast the capacity reduction for real sectors in Munich airspace.

3.3.2 Rhein UIR Airspace Model

The airspace is a right three-dimensional prism. Following [19], we define an altitude band as a 1000ft-high horizontal slice of the airspace, centered on a flight level. Figure *8*The bases of the band prism belong to the upper and lower boundaries of a band. The airspace is split into sectors, each of which is composed of band prisms stacked one on top of one another. Thus, the cross-section of a sector by any horizontal plane within an altitude band is constant. We identify the sector at the flight level with the cross-section polygon. The geometry of the airspace sectors may be different at different altitudes.

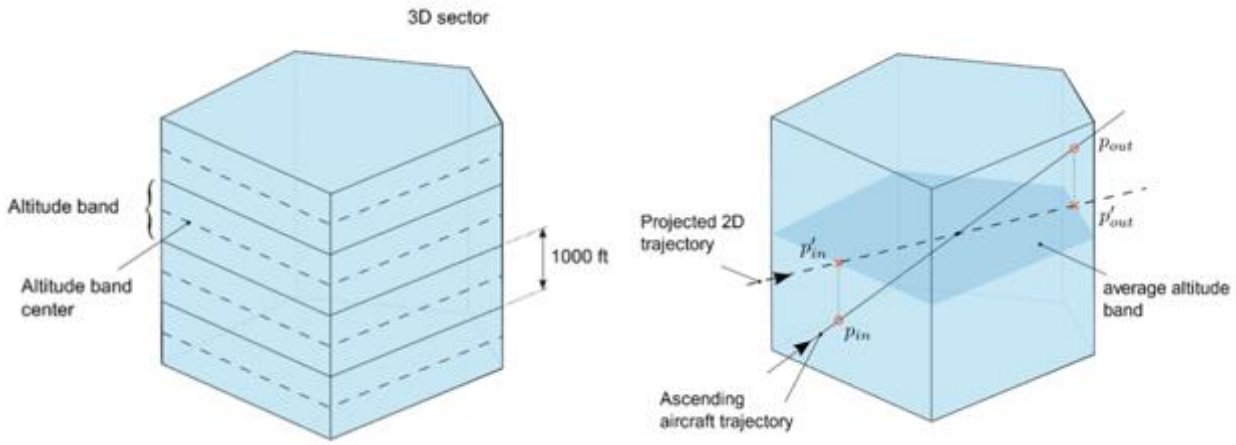

Figure 8 - Left: Altitude bands. Right: The entry and exit points are projected onto the altitude band corresponding to the average of the entry and exit altitudes.

Hazardous weather cells are treated as three-dimensional obstacles to be avoided by the aircraft. The weather obstacles are provided for each timestep over a given time horizon. A weather obstacle is a right prism, defined by a polygon and a vertical extent. The upper and lower bases of every obstacle are defined by an altitude band, i.e., no obstacle starts or ends inside an altitude band. This way, for a particular prediction time and an ensemble member, the hazardous weather at each altitude is a set of polygons (see the example in Figure 7).

The weather data is provided by the thunderstorm tracking, monitoring and nowcasting tool called Cb-Global, which is based on Cb-TRAM (Cumulonim Bus TRacking And Monitoring) developed by DLR [20]-[22]. Cb-TRAM operates on multi-channel information from the SEVIRI (Spinning Enhanced Visible and Infrared Imager) instrument onboard the Meteosat Second Generation (MSG) geostationary satellite [23]. Deterministic nowcasting identifies three consecutive development stages: (i) local early development, (ii) rapid growth and (iii) mature deep convection. A short-term forecast (up to 1 hour) is produced from Lagrangian extrapolation along atmospheric motion vectors computed with the pyramidal image matcher. Cb-TRAM is specifically developed for aviation and was used in several studies [24][26]. In this case, the mature convection polygons produced by Cb-Global, enlarged were used as Weather Avoidance Fields (WAFs).

The demand for a sector during a time of interest is defined by the number of aircraft that plan to pass through the sector. The flight plan for any aircraft is a sequence of 4D waypoints (location and time). Using the definition from [19], each flow is identified by a sector transit triplet: entry sector, current sector, and exit sector.

An example is depicted in the right side of Figure 7, where three different flows through the EDUUUTAS airspace are shown: flow 1 (black) corresponds to the transit triplet EDUUUTAW-EDUUUTAS-LOVVCTA; flow 2 (light-green) corresponds to the triplet EDUUUTAE-EDUUUTAS-LOVV1CTA; and flow 3 (blue) corresponds to the triplet LSAZUTA-EDUUUTAS-LKAACTA. We calculate the capacity for every pair of entry/exit airspace/sector through which the traffic intends to go. The number of aircraft in each flow is determined by identifying the sector entry and exit 4D points (time and location) of the aircraft trajectories, as well as the origin and destination adjacent sectors. Following [17], ascending or descending aircraft are treated as if they fly level at an average altitude.

3.3.3 Airspace Capacity Impact Calculation

The metric of choice to evaluate the weather-impacted airspace capacity is the prediction of available sector capacity ratio (ASCR) for each time of consideration, which is the ratio of the sector capacity under the given weather constraints (Wmincut) to the maximum possible capacity of the sector without weather systems (Omincut). The ratio ranges between 0 and 1, where 0 represents a completely blocked airspace with no usable capacity and 1 represents an airspace without constraints. Figure 9 shows the example of a flow, a W_{mincut} and an O_{mincut}. This is similar to the permeability metric presented in section 3.1 and in Figure 3. More details on how the ASCR is

calculated can be found in [17].

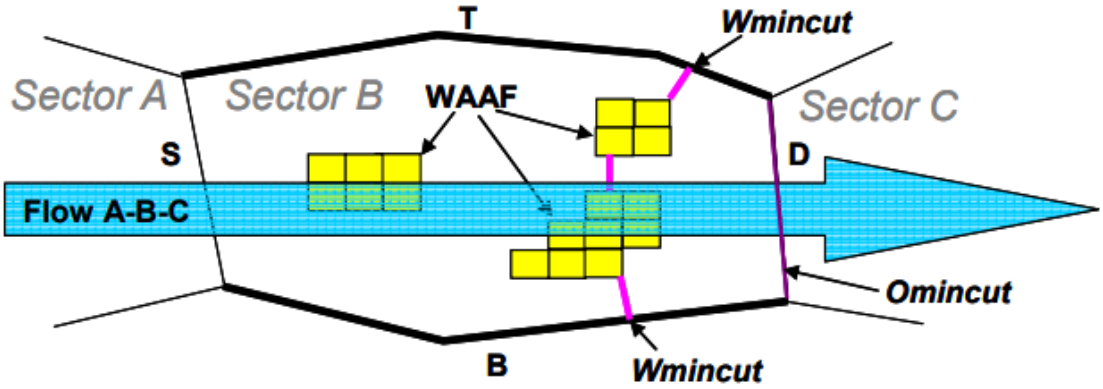

Figure 9 – Simplified representation of the airspace weather impact model described in [17]. Blue arrow represents the main direction of flow, yellow boxes are simplified weather avoidance altitude fields (WAAF), magenta line represents the available airspace to traverse, purple line D represents airspace available to traverse without weather.

Figure 7 presents an example impacted flow (blue dash line) applied for the EDUUUTAS airspace obtained for this study. The ASCR is determined considering the total number of flows at all altitude bands. Figure 10 shows the raw data used as an input for the ASCR calculation in terms of weather and traffic data for the EDUUUTAS airspace.

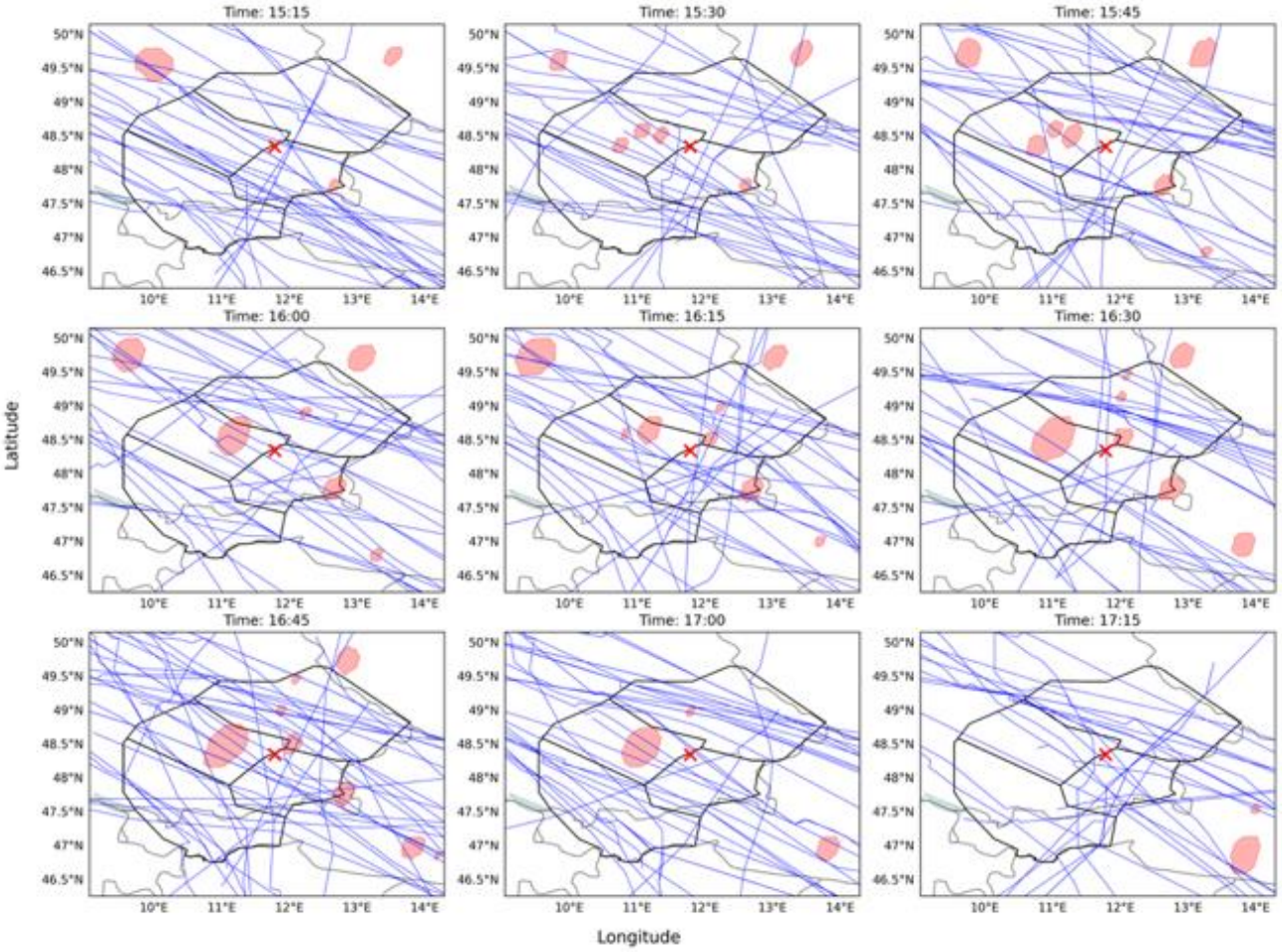

Figure 10 – Traffic routes (blue) and convective weather data (red) in EDUUUTAS during the period studied (1515Z to 1715Z on June 8, 2023) on a quarter hourly basis. Only routes for those flights are shown, which are present within the sector group at the dedicated time.

3.3.4 Data & Results

We divide the time interval of interest into the 15-minutes periods and consider the most accurate weather observations and forecast for that time period, i.e. the one with the closest time to the prediction. The historical flight plans over the EDUUUTAS airspace for the selected times were obtained from Eurocontrol's DDR2 repository [27]. Vertically, the airspace is divided into the 1000ft-high horizontal slices, ranging between the FL315 and FL600, with 42 flows identified in each of them. The resulting ASCR for the period of consideration is shown in Figure 11.

Similarly to the case presented in section 3.1, the weather causes a significant reduction in the airspace capacity, with the lowest capacity around 16:30 (ASCR=0.47, when the average airspace capacity is half than in the airspace free of weather obstacles). Nonetheless, differently from the case in Florida, the capacity reduction only lasts for about one hour, returning to 100% at the end of the period analyzed.

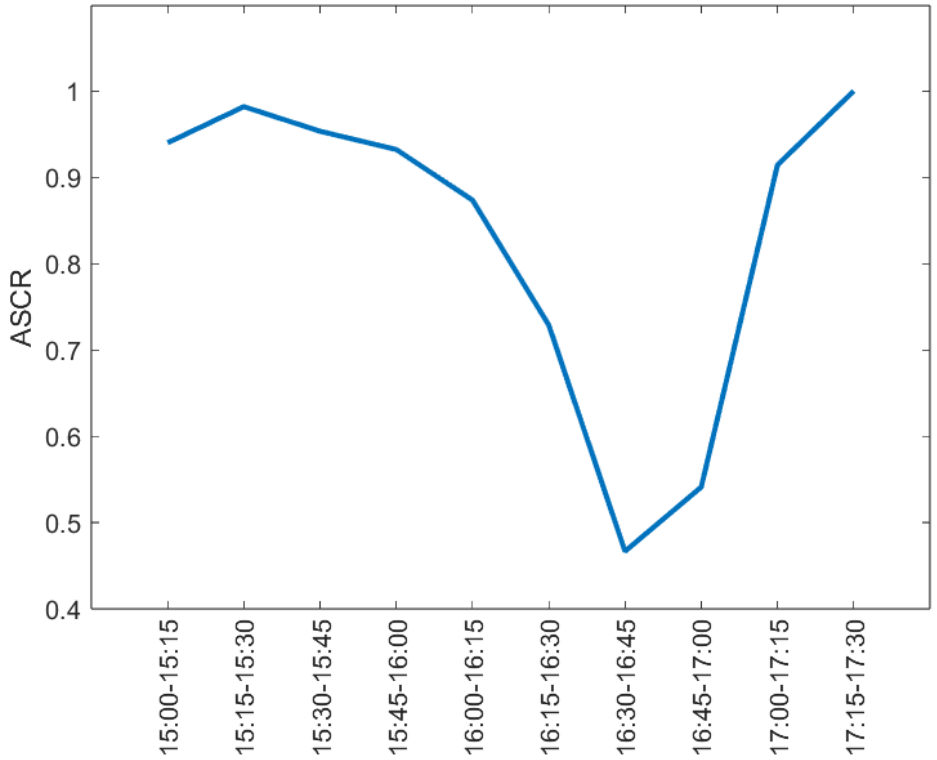

Figure 11 - ASCR for EDUUUTAS ACC over Munich airport on June 8, 2023.

4. Summary and Conclusions

In this paper, three case studies were presented to illustrate weather impact models that are currently used in DSTs in the United States and Canada and that were developed for this study for the airspace around Munich Airport in Europe.

From the case studies presented in this paper, it is clear that different models can be used to predict the impact of convective weather cells on airspace capacity. Each model, with different maturity levels, predicts what is the capacity reduction at what time. This information is necessary for traffic managers to plan airspace or airport programs (regulations in Europe) to strategically mitigate the effects of the weather impacts. Key decisions that these models can support are when to start a program, how long the program needs to last, and when to end it. Exit strategies are paramount to make sure that the demand is not overly constrained making the recovery of traffic too slow or impossible.

Busy airports and airspace around the world are similarly impacted by convective weather but advanced weather models have the potential to support traffic managers and therefore reduce the impact of these events. This study has shown three compelling examples of such applications. Future developments can be envisioned go even further, for example by translating weather impacts into programs flow rates with uncertainty bounds to leave the final decision to the traffic managers

but to provide the minimum and potential maximum predicted impact. This work is intended to start to compare and contrast weather challenges between the different regions considered, identify and share technologies and best practices to mitigate them, and help move towards a more globally harmonized air traffic management system.

1. Contact Author Email Address

Contact author: gabriele.enea@ll.mit.edu

2. Copyright Statement

References

[1] Bureau of Transportation Statistics, *Causes of National Aviation System Delays 2022*, URL: https://www.transtats.bts.gov/OT_Delay/OT_DelayCause1.asp?20=E

[2] Taszarek, M., et al., Severe Convective Storms across Europe and the United States”. *Journal of Climate*, 33(23), pp.10263-10286, 2020.

[3] Rozario, L., “Clear Aviation”, In *Meteorological Technology International*, September 2023, URL: https://www.ukimediaevents.com/publication/b9b99838.

[4] EASA, Appendices to EASA *Scientific Committee Annual report 2022*.

URL: https://www.easa.europa.eu/en/domains/research-innovation/easas-scientific-committee-scicomm

[5] Enea, G., Dean, R., Knorr, D., ”Pre/Post COVID: Major Changes in Florida Demand & FAA’s Traffic Management Response”, *Transportation Research Board (TRB) Annual Meeting, Washington, DC, 2024.*

[6] Matthews, M., Veillette, M., Venuti, J., DeLaura, R., Kuchar, J., “Heterogeneous Convective Weather Forecast Translation into Airspace Permeability with Prediction Intervals”, *Journal of Air Transportation,* Vol. 24, No,. 2, April 2016.

[7] FAA, ASPM Website, URL: https://aspm.faa.gov/aspmhelp/index/Aviation_System_Performance_Metrics_(ASPM).html

[8] Reynolds, T., Matthews, M., Enea, G., Cushnie, B., “Weather-Aware Integrated Air Traffic Management Technology Development”, *SESAR Innovation Days*, Seville, Spain, 2023.

[9] Enea, G., Lau, A., Pawlak, M., Reynolds, T., Knorr, D., Durbin, M., Roth., P., Schwanke, S., Dussoye, S., “Evaluation of Convective Weather Impacts on US and European Airports”, *15th FAA/EUROCONTROL ATM R&D Seminar,* Savannah, GA, 2023.

[10] Lemetti, A., Polishchuk, T., Polishchuk, V. Valenzuela, A. Franco, A. Nunez-Portillo, J. Rivas, D., ”Probabilistic Analysis of Airspace Capacity in Adverse Weather Scenarios”. *SESAR Innovation Days*, Budapest, Hungary, 2022.

[11] Polishchuk , V., Mitchell, J., “Thick Non-Crossing Paths and Minimum-Cost Flows in Polygonal Domains”, *Proceedings of the Twenty-Third Annual Symposium on Computational Geometry,* New York, NY, 2007.

[12] Arkin, E. M. Mitchel J. S. B. , Polishchuk, V. “Maximum thick paths in static and dynamic environments,» *Computational Geometry,* vol. 43, pp. 279-294, 2010.

[13] Kim, J. Mitchell, J. S. B. Polishchuk, V., Yang, S., Zou, J., “Routing multi-class traffic flows in the plane”, *Computational Geometry,* vol. 45, pp. 99-114, 2012.

[14] Eriksson-Bique, S. Polishchuk V., Sysikaski, M. "Optimal Geometric Flows via Dual Programs," in *Proceedings of the Thirtieth Annual Symposium on Computational Geometry*, New York, NY, USA, 2014.

[15] Krozel, J. “Maximum Flow Rates for Capacity Estimation in Level Flight with Convective Weather

Constraints", *Air Traffic Control Quarterly,* vol. 15, 7 2007.

[16] Yang, S. Mitchell, J. S. B. Kim, J. Zou, J. Krozel, J. Polishchuk, V., "Flexible Airlane Generation to Maximize Flow under Hard and Soft Constraints", *Air Traffic Control Quarterly,* vol. 19, pp. 211-235, 2011.

[17] Song, L. Wanke, C. Zobell, S. Greenbaum D. Jackson, C. "Methodologies of Estimating the Impact of Severe Weather on Airspace Capacity", *The 26th Congress of ICAS and 8th AIAA ATIO,* Anchorage, AK, 2008.

[18] Steiner, M. Bateman, R. Megenhardt, D. Liu, Y. Xu, M. Pocernich, M. Krozel, J. "Translation of Ensemble Weather Forecasts into Probabilistic Air Traffic Capacity Impact", *Air Traffic Control Quarterly,* vol. 18, pp. 229-254, 2010.

[19] Song, L. Wanke, C., Greenbaum, D. Callner, D. "Predicting Sector Capacity under Severe Weather Impact for Traffic Flow Management", *7th AIAA ATIO Conference, 2nd CEIAT International Conference on Innovation and Integration in Aero Sciences,17th LTA Systems Tech Conf; followed by 2nd TEOS Forum;* 2007.

[20] Zinner, T. Mannstein, H. Tafferner, A.,"Cb-TRAM: Tracking and monitoring severe convection from onset over rapid development to mature phase using multi-channel Meteosat-8 SEVIRI data". *Meteorology and Atmospheric Physics*, 101, 191-210, 2008.

[21] Merk, D.,Zinner, T., "Detection of convective initiation using Meteosat SEVIRI: Implementation in and verification with the tracking and nowcasting algorithm Cb-TRAM. Atmospheric Measurement Techniques, 6(8), 1903-1918, 2013.

[22] Zinner, T. Forster, C. De Coning, E. Betz, H. D., "Validation of the Meteosat storm detection and nowcasting system Cb-TRAM with lightning network data–Europe and South Africa", *Atmospheric Measurement Techniques*, 6(6), 1567-1583, 2013.

[23] Schmetz, J. Pili, P. Tjemkes, S. Just, D. Kerkmann, J. Rota, S., Ratier, A., "An introduction to Meteosat second generation (MSG)",. *Bulletin of the American Meteorological Society*, 83(7), 977-992, 2002.

[24] Forster C., Tafferner, A., "Nowcasting thunderstorms for Munich airport", *The DLR Project Wetter & Fliegen*.

[25] Forster, C., Ritter, A., Gemsa, S. Tafferner, A. Stich, D., „Satellite-based real-time thunderstorm nowcasting for strategic flight planning en route", *Journal of Air Transportation*, 24(4), 113-124, 2016.

[26] Lau, A., Forster, C., Tafferner, A., Dzikus N., "Assessment of a Weather Nowcasting and Tracking Algorithm Based on Delay Reduction Potential at Munich Airport (Part I)", *11th AIAA Aviation Technology, Integration und Operations (ATIO)*, Virginia Beach, VA, 2011.

[27] EUROCONTROL. DDR2 Reference Manual for General Users 2.9.4, 2017.